PHYSICAL REVIEW B VOLUME 24, NUMBER 4 15 AUGUST 1981

Local-field effects and the ir optical properties of ternary semiconductor alloys

R. Bonneville
Centre National d'Etudes des Télécommunications, * *196 rue de Paris, 92220 Bagneux, France*

(Received 10 February 1981)

We present a calculation of the infrared dielectric function of a three-dimensional ternary semiconductor alloy $AB_{1-x}C_x$. The diagonal disorder (masses) is treated in the coherent potential approximation; the off-diagonal disorder (force constants) as well as all the electronic properties (background dielectric constant, electronic screening) is handled by the virtual-crystal approximation. We use a nearest-neighbor single-force-constant potential which is shown to be sufficient to account for the optical properties. With the data of $Ga_{1-x}Al_xAs$, the calculated density of states shows one acoustic band and two optical bands, one near the gap mode of Ga in AlAs, and the other near the localized mode of Al in GaAs. Particular attention has been given to the local-field effects caused by the ionic and electronic polarization and by the screening due to the electronic delocalization. The line broadening induced by the disorder forces one to make a precise definition of the longitudinal and transverse frequencies. In addition to the well-known two-mode behavior of $Ga_{1-x}Al_xAs$, the model predicts a third very weak mode (about a hundred times weaker), which is a disorder-activated zone-edge mode. The model also predicts a rapid variation of the longitudinal-transverse splitting of the two main modes when one approaches the pure-crystal limit. The numerical results agree well with the experimental data and are also compared with those of the linear diatomic chain.

I. INTRODUCTION

Since the celebrated textbook by Born and Huang was published,[1] a considerable amount of work has been devoted to the dynamics of crystal lattices and to the interpretation of their optical ir or Raman properties. Theoretical concern as well as applications in view have led people to investigate the effects linked to the presence of defects inside an ordered medium. Henceforth, we shall be interested in the changes in the vibrational modes and in the infrared spectrum due to the random substitution in a lattice—and more particularly in a diatomic crystal—of one type of atom by another miscible isoelectronic species belonging to the same column of the Periodic Table.

It is well known that the optical properties of the mixed crystals $AB_{1-x}C_x$ usually show either a so-called one-mode or a two-mode behavior.[2] In the latter case, a longitudinal-transverse (LT) multiplet coinciding with that of the pure AB crystal when $x=0$ evolves roughly linearly with the concentration of C towards the localized mode of a B atom in the AC crystal when $x=1$, simultaneously the LT splitting and the intensity decrease to 0. For the other mode the results are reversed. In the one-mode behavior, the LT multiplet of the pure AB crystal evolves towards the LT multiplet of the AC crystal. Some crystals evidence both kinds of behavior in different concentration ranges.

The behavior of an otherwise perfect diatomic chain when a single atom has been substituted by an isotope is well known and is characterized by the emergence of new resonance modes:

(i) One substitutes a heavy atom of mass M by an isotope of mass M^*: If $M^*>M$, no extra resonant frequency appears; if $M^*<M$, two new modes are revealed, a gap mode originating from the top of the acoustic band and a localized mode originating from the top of the optical band.

(ii) A lighter atom of mass m is replaced by an atom of mass m^*: If $m^*>m$, a gap mode originating from the bottom of the optical band appears; if $m^*<m$, a localized mode comes out from the top of the optical band.

More generally, the properties of an isotopically substituted linear diatomic chain have been extensively studied by Maradudin and co-workers.[3] However, though the changes due to the force constants modifications are much less important than those due to the mass changes, the above results are not always sufficient to predict the behavior of an actual three-dimensional crystal.

Such simple models as the random element isodisplacement (REI) model (Chang and Mitra[4]) provide us with useful information, such as criteria for having single-mode or two-mode behavior, and the dependence on the concentration of the optical modes if one knows the properties of the pure crystals AB and AC. However, those models cannot give information about the intensity, linewidth, and resonance profile, just as any model dealing with a finite number of infrared-active modes cannot. The simplest way to obtain such information is to fit the experimental data for the dielectric constant by a one or two damped oscillators model, in the latter case possibly coupled by local-field effects. The actual alloy problem is that of an infinite number of oscillators in the continuum limit (one for each value of the wave vector $\vec{k}$), decoupled in the perfect crystal, but coupled by the mass-disorder perturbation in the alloy. Every mode of the perfect crystal then gains a small $\vec{k}=\vec{0}$ component (only the $\vec{k}=\vec{0}$ component is coupled to the light) and thus contributes to the dielectric properties. The local-field effects also couple these contributions together. Furthermore, nothing forbids the occurrence of other resonance peaks besides the one or two mode behavior; indeed, such resonances interpreted as originating from the zone-edge modes are actually observed.

The Green-function formalism, initiated for this kind of problems by Maradudin *et al.*,[3] Mazur *et al.*,[5] and Montroll *et al.*,[6] is well suited for treating the real alloy as a perturbation of the perfect crystal; the propagator of the former can be expressed as a Dyson series of the propagator of the latter and of the perturbation.[7] The perturbative treatment, i.e., truncating the Dyson expansion, leads to increasing difficulties with the order of perturbation. Also, if one only retains first- or second-order terms in perturbation (i.e., in concentration) the agreement with the experimental data is good only for very low concentrations. Moreover, the truncating procedure does not preserve the number of degrees of freedom in the system and can lead to unphysical results, e.g., an unormalized density of states. A mean-field (MF) model does not have these disadvantages; the simplest MF model, viz., the virtual-crystal approximation (VCA), and the more elaborate approximate-transition-matrix approximation (ATA) provide us with good results for low concentrations only as we shall recall later on. The most powerful tool, though not too heavy to handle, is the coherent potential approximation[8] (CPA). It can be applied even for high defect concentrations, since it allows to sum in a self-consistent way the greatest number of elementary processes. This method has been initiated by Taylor for one- and three-dimensional binary alloys[9]; compared with the numerical simulations by Dean of the linear chain,[10] it accounts fairly well for the low-frequency modes (long-range order), but smears out the complex fine structure of the localized modes (cluster effects). This method has then been used by Sen and Hartmann to compute the density of states and the polarizability of a one-dimensional diatomic chain as a model of a ternary alloy.[11] Kaplan and Mostoller[12] have developed accurate numerical techniques which make quasiautomatic the CPA procedure for mass defects in monatomic cubic crystals, and greatly facilitate the calculation in the case of polyatomic cubic compounds; however, in the latter case, the computation requires an important amount of time. As a starting point, one has to know the dynamic matrix and thus the density of states of a perfect crystal used as a reference. Inasmuch as the CPA calculation is correct up to third-order terms with respect to the mass-defect perturbation,[13] one can be content for the reference density of states with an approximate function which correctly reproduces the three first moments only.

One of the two purposes of this paper is to present a CPA calculation of the density of states and of the susceptibility of a three-dimensional ternary alloy; however, performing simplifying assumptions so as to make the numerical procedure easier:

(i) The off-diagonal disorder (force constants) as well as all the other electronic properties (background dielectric constant, screening factor, effective charges) will be treated in the VCA, i.e., a mere linear interpolation; conversely, the diagonal disorder (masses) is accounted for in a CPA procedure. The experimental data we use are those for $Ga_{1-x}Al_xAs$. The pure compounds GaAs and AlAs have the same cell parameter to within 1%, and nearly equal effective force constants and background dielectric constants; in those alloys, the disorder effects are clearly due to the mass difference of the two cations. In any case the modifications due to the force constant changes are far less important than those due to the mass changes.

(ii) We assume only one force constant in the model, giving triply-degenerate bands. This assumption may look rough. However, it is a quite reasonable one since we are mainly interested in the optical properties. The agreement with the optical data justifies it *a posteriori*. Besides the known two-mode behavior of $Ga_{1-x}Al_xAs$, the model predicts a third mode, very weak (about one hundred times weaker) whose intensity, position, and linewidth do not vary much for concentrations between 0.1 and 0.9; this additional mode corresponds to a disorder activated acoustic mode near the zone edge.

The second purpose of this article is to try to clarify some points concerning local-field effects and elementary excitations. It is easy to realize that the polarizability of a classical harmonic oscillator and that of a quantum one are identical when no damping occurs (in the case of a phonon, the purely radiative damping is completely negligible) and we shall also neglect the anharmonicity. On another hand, when one deals with localized charge distributions (phonons or Frenkel excitons), quantum theory is necessary only for calculating the polarizability of the elementary excitations, but not for handling the local-field effects. For instance, the results of Hopfield's calculation of the long-range exciton-exciton interaction are strictly identical to those of a classical local-field treatment. In the case of such a randomly disordered medium as an alloy, instead of dealing with a one or two oscillators model, the CPA model allows one to handle the problem of a continuum of classical oscillators, coupled together by the local-field effects and by the disorder. It is then attractive in such a case where the resonance lines appear shifted and broadened to reexamine such notions as the longitudinal and transverse frequencies and the Lyddane-Sachs-Teller relation, and the polariton effect.

One can deduce from Born and Huang's textbook the following relation between the longitudinal frequency ω_L, the transverse frequency ω_T, the high-frequency dielectric constant ϵ_∞, and the optical-phonon frequency $\omega_\mu^2 = 2K/\mu$ ($2K$ is the effective short-range force constant; μ is the reduced mass),

$$\epsilon_\infty \omega_L^2 + 2\omega_T^2 = (\epsilon_\infty + 2)\omega_\mu^2 .$$

There is still a great confusion in the literature about this point: Instead of the above relation, a number of authors take $\omega_T = \omega_\mu$, an equality which should hold only if one neglects the local-field effects. A similar problem arises in the case of excitonic polaritons in semiconductors when separating short-range terms (exchange interaction) and long-range terms (local-field effects): As analyzed in Ref. 14, some contradictory relations are simultaneously used. In a semiconductor where the high-frequency dielectric constant ϵ_∞ is of the order of 10, this can lead to serious troubles. In addition to the effects included in the treatment of Born and Huang, the present model accounts for the screening of the ionic charge by the delocalization of the electronic distribution through the screening factor γ discussed in Ref. 14, and attempts to clarify the notion of effective charge. We shall assume that the As atoms bear an unscreened charge $-Ze$, and that the Ga and Al atoms have the same charge $+Ze$; however, the effective (screened) polarizability ξ will be different in GaAs and AlAs, due to a different screening factor. The only parameters needed in the calculation are those relative to pure GaAs and AlAs. This model predicts a very rapid decrease of the LT splitting between $x=0$ and $x=0.1$, and between $x=1$ and $x=0.9$, for the principal modes as well as for the localized modes, as observed in quite recent Raman scattering experiments; it also provides us with information about the linewidths and the resonance profiles.

In the following sections, we shall first recall briefly a simple presentation of the CPA procedure in the Lagrangian form, and we shall then present the dielectric properties of the alloy including the local-field effects. In Sec. IV we shall report the results of a one-dimensional model, and in Sec. V, those of the three-dimensional case. The former calculation gives the qualitative tendancies; however, it involves spurious singularities. The calculation for the three-dimensional case eliminates these singularities and gives significantly better results.

II. THE CPA MODEL FOR PHONONS

In this section we briefly recall how the vibrational properties of an alloy can be handled by the CPA procedure. Further details can be found in Refs. 8–13. In the harmonic approximation, the system is described by the Lagrangian

$$L = \tfrac{1}{2}\sum_{i=1}^{\mathfrak{N}} m_i \dot{q}_i^2 - \tfrac{1}{2}\sum_{i=1}^{\mathfrak{N}} K_{ij} q_i q_j ,$$

where q_i is the atomic coordinate and $\mathfrak{N}$ is the number of degrees of freedom of the system. Introducing the $\mathfrak{N}\times\mathfrak{N}$ diagonal mass matrix $M_{ij} = m_i \delta_{ij}$, the $\mathfrak{N}\times\mathfrak{N}$ force constant matrix K_{ij}, and the column vector $Q=\{q_i\}$, the equations of motion are written as

$$M\cdot\ddot{Q}(t) + K\cdot Q(t) = 0 .$$

The Green function $\mathcal{G}(t)$ of the Lagrange equations is defined by

$$M\cdot\ddot{\mathcal{G}}(t) + K\cdot\mathcal{G}(t) = -I\delta(t-t_0)$$

(I being the identity matrix), and its Fourier transform $G(\omega)$ is readily obtained as

$$G(\omega) = \frac{I}{M(\omega^2 + i0^+) - K} . \tag{1}$$

The eigenfrequencies ω_p are the poles of G, i.e., the roots of the secular equation $\det(M\omega^2 - K) = 0$. If the system is subjected to an external force, its contribution to the Lagrangian is

$$L_{\text{ext}} = \sum_i f_i q_i = F\cdot Q .$$

The linear response of the system at the frequency ω of the external field is given by

$$Q = -G(\omega)\cdot F . \tag{2}$$

In the normal mode basis, $\mathrm{Tr}(MG)$ is equal to $\sum_p 1/(\omega^2 - \omega_p^2)$. Using the relation

$$\frac{1}{x+i0^+} = V_p\left(\frac{1}{x}\right) - i\pi\delta(x) ,$$

one finds

$$\sum_{p}\frac{1}{\omega^2+i0^+-\omega_p^2}=V_p\left(\sum_{p}\frac{1}{\omega^2-\omega_p^2}\right)-i\pi\sum_{p}\delta(\omega^2-\omega_p^2)\,.$$

In the continuum limit ($N\rightarrow\infty$) the δ-function term is the density of states $D(\omega^2)$ so that one obtains the density of states

$$\rho(\omega)=-\frac{2\omega}{\pi}\mathrm{Im}[\mathrm{Tr}(MG)]\,. \tag{3}$$

If the system is perturbated by an isotopic substitution, then L is transformed into $L+\Delta L$, with

$$\Delta L=\sum_{i}\tfrac{1}{2}(m_i^*-m_i)\dot{q}_i^2=\tfrac{1}{2}\Delta M:\dot{Q}\dot{Q}\,,$$

the new eigenfrequencies of the systems are the solutions of

$$(M\omega^2-K)\cdot Q=-\omega^2\Delta M\cdot Q\,.$$

Let G_0 and G be the Green functions of the unperturbated and perturbated system respectively, i.e.,

$$G_0=(M\omega^2-K)^{-1}\,,\quad G=[(M+\Delta M)\omega^2-K]^{-1}\,.$$

G and G_0 are easily seen to be connected by the Dyson equation[15]

$$G=G_0+G_0\Lambda G \tag{4}$$

with $\Lambda=-\omega^2\Delta M$, which can be expanded between the sites i and j as

$$G^{ij}=G_0^{ij}+G_0^{ik}\Lambda_{kk}G_0^{kj}+G_0^{ik}\Lambda_{kk}G_0^{kl}\Lambda_{ll}G_0^{lj}+\cdots\,. \tag{5}$$

Λ_{kk} describes the scattering of an eigenmode by the perturbating potential $-\omega^2(m_k^*-m_k)$ attached to the site k. In a first step, we sum up the self-scattering terms so as to evidence the renormalized perturbation,

$$t_{kk}=\Lambda_{kk}+\Lambda_{kk}G_0^{kk}\Lambda_{kk}+\Lambda_{kk}G_0^{kk}\Lambda_{kk}G_0^{kk}+\cdots\,,$$

i.e.,

$$t_{kk}=\frac{\Lambda_{kk}}{1-\Lambda_{kk}G_0^{kk}}\,. \tag{6}$$

We can now write again Eq. (5) as

$$G^{ij}=G_0^{ij}+G_0^{ik}t_{kk}G_0^{kj}+G_0^{ik}t_{kk}G_0^{kl}t_{ll;l\neq k}G_0^{lj}+\cdots\,. \tag{7}$$

This is absolutely general. We come now to adequate physical hypotheses to transform Eq. (6) into a tractable model.

We shall consider any realization $\{r\}$ of the alloy as a perturbation of a fictitious perfect crystal, the sublattice A of which is occupied by fictitious atoms whose mass $\tilde{m}$ is to be determined. Let $G_{(r)}$ be the Green function describing the realization $\{r\}$ of the alloy, and $\tilde{G}_0$ that of the fictitious crystal. In the real alloy, a site i of the sublattice A is occupied by an atom of mass m, and thus is affected by an effective perturbation

$$t_{ii}^{(r)}=\frac{\Lambda_{ii}}{1-\Lambda_{ii}\tilde{G}_0^{ii}}\,,$$

with

$$\Lambda_{ii}=-\omega^2(\tilde{m}-m_i)$$

so that one has

$$G_{(r)}=\tilde{G}_0+\tilde{G}_0t_{kk}^{(r)}\tilde{G}_0+\tilde{G}_0t_{kk}^{(r)}\tilde{G}_0t_{ll;l\neq k}^{(r)}\tilde{G}_0+\cdots\,. \tag{8}$$

We assume that the original atoms and the substituted ones are randomly distributed over the sites of the sublattice A, and we perform a mean-field approximation, i.e., we replace $t_{kk}^{(r)}$ by its average value over all the realizations of the alloy

$$G_{MF}=\tilde{G}_0+\tilde{G}_0\langle t_{kk}^{(r)}\rangle\tilde{G}_0+\tilde{G}_0\langle t_{kk}^{(r)}\rangle\tilde{G}_0\langle t_{ll;l\neq k}^{(r)}\rangle\tilde{G}_0+\cdots\,. \tag{9}$$

The CPA condition for the fictitious crystal to fit as well as possible any realization of the alloy is written as

$$\langle t^{(r)}\rangle=0\,.$$

Equation (9) then reduces to $G_{MF}=\tilde{G}_0$, and averaging both sides of Eq. (8) one obtains[12]

$$\langle G_{(r)}\rangle=\tilde{G}_0+O(t^4)\,. \tag{10}$$

So, the average propagator of the crystal is equal to the propagator of the average crystal up to third-order terms.

We look for perfect-crystal symmetry-adapted (i.e., plane-wave) solutions of the equations of motion. For the ith displacement coordinate of an atom located in $\vec{\mathrm{R}}_p$ on the sublattice X, one has

$$q_i=\frac{1}{\sqrt{N}}\sum_{\vec{\mathrm{k}}}\zeta_i(\vec{\mathrm{k}})e^{i\vec{\mathrm{k}}\cdot\vec{\mathrm{R}}_p}\,.$$

We thus replace the direct-space Green function $G(R_i,R_j,\omega)$ by the reciprocal-space Green function $G(\vec{\mathrm{k}},\vec{\mathrm{k}}',\omega)$, which is more convenient to handle since the propagator G_0 between a state $\vec{\mathrm{k}}$ of the sublattice X and a state $\vec{\mathrm{k}}'$ of the sublattice X' is merely

$$\langle\zeta(\vec{\mathrm{k}})\,|\,G_0\,|\,\zeta'(\vec{\mathrm{k}}')\rangle=\delta_{\vec{\mathrm{k}},\vec{\mathrm{k}}'}\langle\zeta\,|\,G_0(\vec{\mathrm{k}})\,|\,\zeta'\rangle\,.$$

The CPA equations are then written as

$$\langle G_{(r)}(\vec{\mathrm{k}}',\vec{\mathrm{k}},\omega)=\delta_{\vec{\mathrm{k}},\vec{\mathrm{k}}'}\tilde{G}_0(\vec{\mathrm{k}},\omega)\,,$$

$$\langle t^{(r)}\rangle=0\,,$$

with

$$t_{ii}=\frac{\Lambda_{ii}}{1-\Lambda_{ii}\frac{1}{N}\sum_{\vec{\mathrm{k}}}\tilde{G}_0(\vec{\mathrm{k}},\omega)}\,.$$

This approximation thus involves a major simplification since the Green function $G(\vec{k},\vec{k}',\omega)$ becomes diagonal in $\vec{k}$, and $G(\vec{k},\omega)$ is reduced to a $Zl\times Zl$ matrix (Z is the number of atoms in the unit cell and l the dimensionality of the problem).

We now consider the more specific case of a diatomic cubic crystal whose basis atoms have the masses m (sublattice A) and M (sublattice B). Let us remember that we are mainly interested in the optical (i.e., near the Brillouin-zone center) properties; hence we use a tight-binding or nearest-neighbor approximation. The coupling constants K_{ij} are taken to be zero if i and j refer to different sites of the same sublattice, and K_{ij} is also zero if the sites i and j are not nearest neighbors. This is quite pertinent, since it is known that the further than nearest neighbors are mainly important for explaining the zone-edge properties, e.g., the flattening of the transverse acoustic modes, but not for the $\vec{k}\simeq\vec{0}$ properties, e.g., the sound velocities. Inasmuch as the interatomic potential is symmetric around the bond axis, it has quite generally an isotropic part and a quadrupolar part

$$V=\tfrac{1}{2}\sum_{j}\sum_{i}\left(I^{(0)}(\vec{r}_i-\vec{r}_j)^2+I^{(2)}\frac{3[(\vec{r}_i-\vec{r}_j)\cdot\vec{u}_{ij}]^2-(\vec{r}_i-\vec{r}_j)^2}{2}\right)\qquad(11)$$

(the first sum runs over all the atoms of one sublattice, and the second one over its ν nearest neighbors; $\vec{r}_i$ and $\vec{r}_j$ are the displacements of the atoms i and j; $\vec{u}_{ij}$ is a unit vector along the i–j bond). The most general solution of Eq. (11) gives correct optical frequencies and sound velocities. As we are mainly interested in the optical properties, we make a further approximation which is neglecting the quadrupolar part in Eq. (11); we thus have a one force-constant model, having one triply-degenerate optical branch and one triply-degenerate acoustic branch.[16] The normal-mode coordinates α (sublattice A) and β (sublattice B) are triply degenerate and the Green function G_0 reduces to a triply-block-diagonal matrix

$$G_0(\vec{k},\omega)=\begin{pmatrix}G_0' & 0 & 0\\ 0 & G_0' & 0\\ 0 & 0 & G_0'\end{pmatrix},$$

with

$$G_0'=\begin{pmatrix}G_0^{aa} & G_0^{ab}\\ G_0^{ba} & G_0^{bb}\end{pmatrix}.$$

Under those assumptions, the Lagrangian can be written

$$\begin{aligned}L={}&\tfrac{1}{2}\sum_{\vec{k}}m\dot{\alpha}(\vec{k})\,\dot{\alpha}(-\vec{k})+\tfrac{1}{2}\sum_{\vec{k}}M\dot{\beta}(\vec{k})\,\dot{\beta}(-\vec{k})\\&-\tfrac{1}{2}I^{(0)}\sum_{\vec{k}}\nu\alpha(\vec{k})\,\alpha(-\vec{k})+\nu\beta(\vec{k})\,\beta(-\vec{k})\\&+\alpha(\vec{k})\,\beta(-\vec{k})\left(\sum_{i=1}^{\nu}\exp(i\vec{k}\cdot\vec{R}_i)\right)\\&+\alpha(-\vec{k})\beta(\vec{k})\left(\sum_{i=1}^{\nu}\exp(-i\vec{k}\cdot\vec{R}_i)\right),\end{aligned}$$

with $\alpha(-\vec{k})=\alpha^*(\vec{k})$ and $\beta(-\vec{k})=\beta^*(\vec{k})$. The 2×2 Green function matrix is

$$G_0'(\vec{k},\omega)=\frac{1}{\Delta(\vec{k})}\begin{pmatrix}-2K+M\omega^2 & -2K\sigma_{\vec{k}}\\ -2K\sigma_{\vec{k}}^{*} & -2K+m\omega^2\end{pmatrix},\qquad(12)$$

with

$$\Delta(\vec{k})=mM\omega^4-2K(m+M)\omega^2+4K^2(1-|\sigma_{\vec{k}}|^2)$$

and

$$\sigma_{\vec{k}}=\frac{1}{\nu}\sum_{i=1}^{\nu}e^{i\vec{k}\cdot\vec{R}_i},\quad 2K=\nu I^{(0)}.$$

The sum in $\sigma_{\vec{k}}$ runs over the ν nearest neighbors of a given atom; in the case of a blende-type lattice, $\sigma_{\vec{k}}$ is merely $\cos(ka/2)$ for a one-dimensional model with period a. In the three-dimensional case, a being the parameter of the conventional cubic cell,

$$\begin{aligned}|\sigma_{\vec{k}}|^2=\tfrac{1}{4}\Bigg[1&+\cos\left(\frac{k_xa}{4}\right)\cos\left(\frac{k_ya}{4}\right)\\&+\cos\left(\frac{k_ya}{4}\right)\cos\left(\frac{k_za}{4}\right)\\&+\cos\left(\frac{k_za}{4}\right)\cos\left(\frac{k_xa}{4}\right)\Bigg].\end{aligned}$$

Henceforth, we shall set

$$\omega_M^2=\frac{2K}{M},\quad \omega_m^2=\frac{2K}{m},\quad \omega_\mu^2=\omega_M^2+\omega_m^2.$$

The eigenfrequencies are

$$\omega^2(\vec{k})=\left(\frac{\omega_M^2+\omega_m^2}{2}\right)\pm\left[\left(\frac{\omega_M^2-\omega_m^2}{2}\right)^2+\omega_M^2\omega_m^2|\sigma_{\vec{k}}|^2\right]^{1/2},$$

the $-$ and $+$ signs refer to the acoustic and optical solutions, respectively. The density of states $D(\omega^2)$ has the behavior shown on Fig. 1. In the

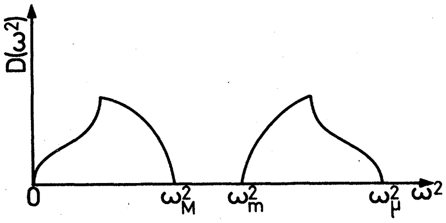

FIG. 1. Behavior of the reference density of states.

presence of an external field, the electromagnetic perturbation in the electric-dipole approximation is

$$L_{\text{ext}}=\sum_{i=1}^{N}(Z_i^a e\vec{r}_i^{\,a}+Z_i^b e\vec{r}_i^{\,b})\cdot\vec{E}$$

$$=Ze\sum_{i=1}^{N}(\vec{r}_i^{\,a}-\vec{r}_i^{\,b})\cdot\vec{E}$$

$$=Ze[\alpha(\vec{0})-\beta(\vec{0})]E\sqrt{N}$$

($\vec{r}_i^{\,a}$ and $\vec{r}_i^{\,b}$ are the displacements of the atoms a and b of the ith cell, Z_i^a and Z_i^b their charges), or $L_{\text{ext}}=V\vec{P}\cdot\vec{E}$ ($\vec{P}$ is the dielectric polarization, and V the total volume). From Eq. (2), one derives

$$\begin{pmatrix}\alpha & (\vec{0})\\ \beta & (\vec{0})\end{pmatrix}=-\begin{pmatrix}G_0^{aa} & G_0^{ab}\\ G_0^{ba} & G_0^{bb}\end{pmatrix}_{(\vec{k}=\vec{0})}\begin{pmatrix}Ze & E\\ -Ze & E\end{pmatrix}\sqrt{N},$$

and thus

$$P=(Ze)^2\frac{N}{V}E(-G_0^{aa}+G_0^{ab}+G_0^{ba}-G_0^{bb})_{(\vec{k}=\vec{0})}\,.$$

The ionic polarizability is then written as

$$\alpha_{\text{ion}}(\omega)=\frac{(Ze)^2}{2K}\left(1-\frac{\omega^2}{\omega_\mu^2}\right)^{-1}, \tag{13}$$

but for convenience, we shall define a dimensionless susceptibility

$$\chi(\omega)=\frac{4\pi}{3}\frac{N}{V}\alpha_{\text{ion}}(\omega)\,. \tag{13$'$}$$

We assume that the atoms of one sublattice A (let us say those of mass $m=m_1$) are partially substituted by other atoms (of mass $m=m_2$). If the atoms 1 and 2 are randomly distributed on the sublattice A (i.e., all the realizations of the alloy are equiprobable) the CPA condition $\langle t^{(r)}\rangle=0$ is written as

$$\frac{x\Lambda_{11}}{1-\Lambda_{11}\tilde{G}_0^{aa}}+\frac{(1-x)\Lambda_{22}}{1-\Lambda_{22}\tilde{G}_0^{aa}}=0\,. \tag{14}$$

with

$$\Lambda_{ii}=\omega^2(\tilde{m}-m_i)$$

and

$$\tilde{G}_0^{aa}=\frac{1}{N}\sum_k\frac{-2K+M\omega^2}{\tilde{m}M\omega^4-2K(M+\tilde{m})\omega^2+4K^2(1-|\sigma_k|^2)}\,.$$

This expression is symmetric in m_1,m_2. If one introduces the average mass $\bar{m}=xm_1+(1-x)m_2$ and henceforth puts $\omega_m=(2K/\bar{m})^{1/2}$, and the reduced variable $Y=\tilde{m}/\bar{m}$, the self-consistent equation expressing the effective mass $\tilde{m}$ as a function of m_1 and m_2 is

$$Y=1-\left(1-\frac{m_1}{\bar{m}}Y\right)\left(1-\frac{m_2}{\bar{m}}Y\right)\omega^2$$

$$\times\frac{1}{N}\sum_k\frac{\omega^2-\omega_M^2}{\omega^4-\omega^2(\omega_M^2+\omega_m^2Y)+\omega_M^2\omega_m^2Y(1-|\sigma_k|^2)}$$

This equation $Y=F(y)$ can be solved iteratively, i.e., $y_n=F(y_{n-1})$; in the case where several stable points can be evidenced, only one, that with a negative imaginary part, has a physical sense as giving a density of states positive and normalized. The 0th order iteration, $Y_0=1$ or $\tilde{m}=\bar{m}$ is the virtual-crystal approximation; $\langle t(Y_0)\rangle$ has poles which correspond to the localized modes of Ga or Al in the virtual crystal. This is the exact solution in the limit $x\to 0$ or $x\to 1$. The first-order iteration $Y_1=F(1)$ is what is called "approximate-t-matrix approximation" (ATA), about which Sen and Lukovsky[17] have shown that it was satisfactory only for very low concentrations. We can then calculate the CPA density of states; one has for the diagonal elements of the Green function

$$G^{aa}(\omega)=\tilde{G}_0^{aa}(\omega)$$

$$=\frac{1}{N}\sum_{\vec{k}}\frac{-2K+M\omega^2}{\tilde{m}M\omega^4-2K(\tilde{m}+M)\omega^2+4K^2(1-|\sigma_{\vec{k}}|^2)}$$

and

$$G^{bb}(\omega)=\tilde{G}_0^{bb}(\omega)$$

$$=\frac{1}{N}\sum_{\vec{k}}\frac{-2K+\tilde{m}\omega^2}{\tilde{m}M\omega^4-2K(\tilde{m}+M)\omega^2+4K^2(1-|\sigma_{\vec{k}}|^2)}, \tag{15}$$

which easily yields for the density of states

$$\rho(\omega)=-\frac{2\omega}{\pi}\text{Im}[\tilde{m}G^{aa}(\omega)+MG^{bb}(\omega)]\,. \tag{16}$$

III. DIELECTRIC PROPERTIES

So far we have only dealt with the mechanical equations of motion, what we can call "short-range" forces. We shall see now how the coupling with the electromagnetic field, and the resulting perturbation induced by the "long-range" forces, i.e., the local-field effects, is achieved.

The macroscopic Maxwell equations in a dielectric medium are readily separated into $\vec{k}$-longitudinal (∥) and $\vec{k}$-transverse (⊥) contributions; hence the electric field E and the polarization P are connected (in Gaussian units) through

$$E_{\parallel}=-4\pi P_{\parallel}\,,$$

$$\left(k^2-\frac{\omega^2}{c^2}\right)E_{\perp}=4\pi\frac{\omega^2}{c^2}P_{\perp} \tag{17}$$

(ω is the frequency, $\vec{k}$ the wave vector, and c the speed of light). The constitutive equation $P = (\epsilon - 1)E/4\pi$, which defines the dielectric function ϵ, thus has two solutions, the longitudinal one $\epsilon_{\parallel} = 0$ and the transverse one $\epsilon_{\perp} = k^2c^2/\omega^2$.

At the center of the Brillouin zone, the optical mode of a diatomic cubic crystal is a triply-degenerate vibration at the frequency ω_μ. The lowering of the symmetry when one leaves the Γ point splits this mode into a doubly-degenerate branch (TO) and a singly-degenerate one (LO). The dispersion curve of the electromagnetic field $\omega = ck$ crosses the dispersion curve of the phonon very close to the center of the Brillouin zone ($k/k_{\max} \sim 10^{-5}$) so that one can admit that the optical mode is still quasidegenerate. In the case of polar crystals (CsCl, NaCl, ZnS), the optical phonon couples with the vacuum electromagnetic field, which generates mixed eigenmodes (polaritons) and removes the quasidegeneracy: Two transverse (TO) twice-degenerate branches are coupled to the electromagnetic field and are separated by a gap between ω_T and ω_L (longitudinal-transverse splitting); one nondegenerate longitudinal (LO) branch is not coupled to the field.

Let us first consider an ir optically-active vibration in a perfect crystal that we shall describe by a classical harmonic oscillator of frequency Ω [N.B., since $\Omega/c \ll 2\pi/a$, we shall neglect the dispersion $\Omega(\vec{k})$ of the optical-phonon branch] with an effective mass m_e, with $\Omega^2 = 2K/m_e$ and an effective charge q_e; its equation of motion can be written

$$m_e\ddot{Q} = -m_e\Omega^2 Q + q_e F \,. \tag{18}$$

Here F is the effective field acting on the oscillator; F is the superposition of the macroscopic field in the medium E and of induced terms; let P_{ion} be the ionic polarization and P_{el} the electronic polarization; in a cubic crystal, F is expressed as

$$F = E + \tfrac{4}{3}\pi P_{\text{ion}} + \tfrac{4}{3}\pi\gamma P_{\text{el}} \,. \tag{19}$$

The delocalization factor γ lies between 0 and 1; for strongly localized electronic charges (e.g., pure molecular or ionic compound) $\gamma \to 1$, whereas in the case of a completely delocalized electronic distribution, $\gamma \to 0$ (e.g., electronic jellium); actual semiconductors form an intermediate case (a more complete analysis is given in Ref. 14). The ionic polarization is given by

$$\begin{aligned} P_{\text{ion}} &= \frac{N}{V}q_e Q \\ &= \frac{Nqe^2}{V\,2K}\frac{1}{1-\omega^2/\Omega^2}F \end{aligned} \tag{20}$$

and the electronic polarization by

$$P_{\text{el}} = \frac{N}{V}\alpha_\infty F \,, \tag{21}$$

α_∞ being the electronic polarizability. One first eliminates the electronic contribution to the induced polarization. At frequencies much higher than the vibration resonance Ω but lower than the electronic transitions, P_{ion} is nearly zero, and P_{el} has such a value P_∞ that

$$P_\infty = \frac{\epsilon_\infty - 1}{4\pi}E = \frac{N}{V}\alpha_\infty(E + \tfrac{4}{3}\pi\gamma P_\infty) \,. \tag{22}$$

α_∞ is thus linked to the high-frequency dielectric constant ϵ_∞ by[18]

$$\tfrac{4}{3}\pi\frac{N}{V}\alpha_\infty = \frac{\epsilon_\infty - 1}{\gamma(\epsilon_\infty - 1) + 3} \,.$$

Introducing Eqs. (21) and (22) into (19), we again write the effective field as

$$F = \frac{\gamma(\epsilon_\infty - 1) + 3}{3}(E + \tfrac{4}{3}\pi P_{\text{ion}}) \,. \tag{23}$$

Writing the total polarization $P = P_{\text{ion}} + P_{\text{el}}$ as $P = (\epsilon - 1)E/4\pi$, and using the expressions Eq. (20) of P_{ion}, (21) and (22) of P_{el}, and (23) of F, we can derive the dielectric function $\epsilon(\omega)$. We are lead to introduce the dimensionless quantity

$$\xi = \tfrac{4}{3}\pi\frac{Nqe^2}{V\,2K}\frac{3 + \gamma(\epsilon_\infty - 1)}{3} \,, \tag{24}$$

which characterizes the effective strength of the phonon-photon coupling (in the case of an ir inactive mode, then $q_e = 0$ and thus $\xi = 0$). The resulting expression of the dielectric function is:

$$\frac{\epsilon - \epsilon_\infty}{\epsilon_\infty + 2} = \frac{\dfrac{\xi}{1-\omega^2/\Omega^2}}{1 - \dfrac{\xi}{1-\omega^2/\Omega^2}} \,. \tag{25}$$

The transverse and longitudinal frequencies ω_L and ω_T are, respectively, solutions of $\epsilon^{-1}(\omega_T) = 0$, $\epsilon(\omega_L) = 0$, thus

$$\omega_T^2 = \Omega^2(1 - \xi) \tag{26}$$

and

$$\omega_L^2 = \Omega^2\left(1 + \frac{2}{\epsilon_\infty}\xi\right) \,, \tag{26$'$}$$

or alternatively one has the two important relations,

$$\epsilon_\infty\omega_L^2 + 2\omega_T^2 = (\epsilon_\infty + 2)\Omega^2 \tag{27}$$

and

$$\omega_L^2 - \omega_T^2 = \frac{\epsilon_\infty + 2}{\epsilon_\infty} \xi \Omega^2 . \tag{27'}$$

More generally, if there is more than one optically-active mode in the crystal, the above calculations can be performed again, and if one introduces the total susceptibility $\chi(\omega) = \sum_i \xi_i / (1 - \omega^2 / \Omega_i^2)$, the dielectric function is finally written as

$$\frac{\epsilon - \epsilon_\infty}{\epsilon_\infty + 2} = \frac{\chi(\omega)}{1 - \chi(\omega)} . \tag{28}$$

When the susceptibility $\chi(\omega)$ is real (no damping), the transverse frequencies ω_T and the longitudinal ones ω_L are still the solutions of $\epsilon^{-1}(\omega_T) = 0$ and $\epsilon(\omega_L) = 0$.

When a strong damping occurs as it is the case in a disordered crystal, one can now define complex transverse and longitudinal frequencies such that $\epsilon^{-1}(z_T) = 0$ and $\epsilon(z_L) = 0$. (In fact, the word "damping" is not quite adequate. Since the Lagrangian was assumed to be quadratic there is no energy transfer to external degrees of freedom, only redistribution among the internal degrees of freedom. However, since the disorder activates the $\vec{k} \neq \vec{0}$ modes and thus generates line broadening, we shall use the term damping when the CPA solution Y has an imaginary part.) The above calculation is still valid, and the expression of z_L and z_T is quite similar to Eqs. (26), i.e.,

$$z_T^2 = \tilde{\omega}_\mu^2 (1 - \xi) ,$$

$$z_L^2 = \tilde{\omega}_\mu^2 \left(1 + \frac{2\xi}{\epsilon_\infty}\right),$$

but one has to keep in mind that now the complex optical frequency $\tilde{\omega}_\mu^2 = \omega_M^2 + \omega_m^2 Y$ proceeds from the CPA calculation. Taking the local-field effects into account changes the polarizability Eq. (13) into

$$\alpha_{\text{ion}}(\omega) = (Ze)^2 \frac{3 + \gamma(\epsilon_\infty - 1)}{3} \times (-\tilde{G}_0^{aa} + \tilde{G}_0^{ab} + \tilde{G}_0^{ba} - \tilde{G}_0^{bb})_{(\vec{k}=\vec{0})} ,$$

and finally the susceptibility Eq. (13′) into

$$\chi(\omega) = \xi \left(1 - \frac{\omega^2}{\tilde{\omega}_\mu^2}\right)^{-1} ,$$

and the dielectric function is still given by Eq. (28). (Let us recall that the background dielectric constant ϵ_∞, the screening factor γ, the force constant K, and thus the effective susceptibility ξ are real and are assumed to vary linearly with the concentration as we go from pure GaAs to AlAs.)

The dielectric function ϵ can also be expressed as

$$\epsilon(\omega) = \epsilon_\infty \frac{z_L^2 - \omega^2}{z_T^2 - \omega^2} ,$$

which yields

$$\text{Im}(\epsilon) = (\epsilon_\infty + 2) \frac{\xi}{1 - \xi} \text{Im}\left(\frac{1}{1 - \omega^2 / z_T^2}\right) , \tag{29}$$

$$\text{Im}\left(-\frac{1}{\epsilon}\right) = \frac{(\epsilon_\infty + 2)}{\epsilon_\infty^2} \frac{\xi}{1 + 2\xi/\epsilon_\infty} \text{Im}\left(\frac{1}{1 - \omega^2 / z_L^2}\right) . \tag{29'}$$

By an analytic continuation, the real transverse frequency ω_T makes Im(ϵ) maximum and positive, and the real longitudinal frequency ω_L makes Im($-1/\epsilon$) maximum and positive also. In our present problem, we can thus define the TO and LO resonances with no ambiguity.

From ϵ' and ϵ'', one can compute the absorption profile or the reflectivity. Let us note that since the total number of degrees of freedom must be conserved, there is a redistribution of the absorption coefficient, but the total oscillator strength is conserved.

IV. ONE-DIMENSIONAL CASE

We have first performed a calculation on a diatomic chain so as to obtain a comparison with the more realistic three-dimensional case. In the one-dimensional case, the summation of Eq. (15) in the continuum limit is straightforward, and the diagonal elements of the CPA Green function are given by

$$\tilde{G}_0^{aa}(z) = \frac{z^2 - \omega_M^2}{\tilde{m}[z^2(z^2 - \omega_M^2)(z^2 - \omega_m^2 Y)(z^2 - \omega_M^2 - \omega_m^2 Y)]^{1/2}}$$

$$\tilde{G}_0^{bb}(z) = \frac{z^2 - \omega_m^2 Y}{M[z^2(z^2 - \omega_M^2)(z^2 - \omega_M^2 Y)(z^2 - \omega_M^2 - \omega_m^2 Y)]^{1/2}} .$$

The determination of the complex square root must be chosen so as to obtain a density of states positive. The CPA equation then results in an algebraic equation of the third degree, which gives one real root and two complex conjugate roots. One only retain the root whose imaginary part is negative, because of causality requirements.

In Table I we have listed the empirical parameters that we have introduced in the calculation.[19] As can be seen in Fig. 2(a), when one varies the Al concentration from 0 to 1, the density of states of the acoustic band evidences no noticeable behavior and is well accounted for by the virtual-crystal model. Conversely, the rest of the spec-

TABLE I. (a) Input parameters (from pure GaAs and AlAs) and (b) derived quantities used in the calculation.

(a)

	m (g)	M (g)	ϵ_∞ (at 10.6 μm)	ω_T (cm^{-1}) (from Ref. 22)	ω_L (cm^{-1}) (from Ref. 22)
GaAs	69.7	74.9	10.9	269	292
AlAs	27.0	74.9	9.6	361	404

(b)

	μ (g)	Ω (cm^{-1}) [Eq. (27)]	$2K$ (g cm^{-2}) [Eq. (12)]	ξ [Eq. (27′)]
GaAs	36.10	287	2.97×10^6	0.115
AlAs	19.85	398	3.13×10^6	0.180

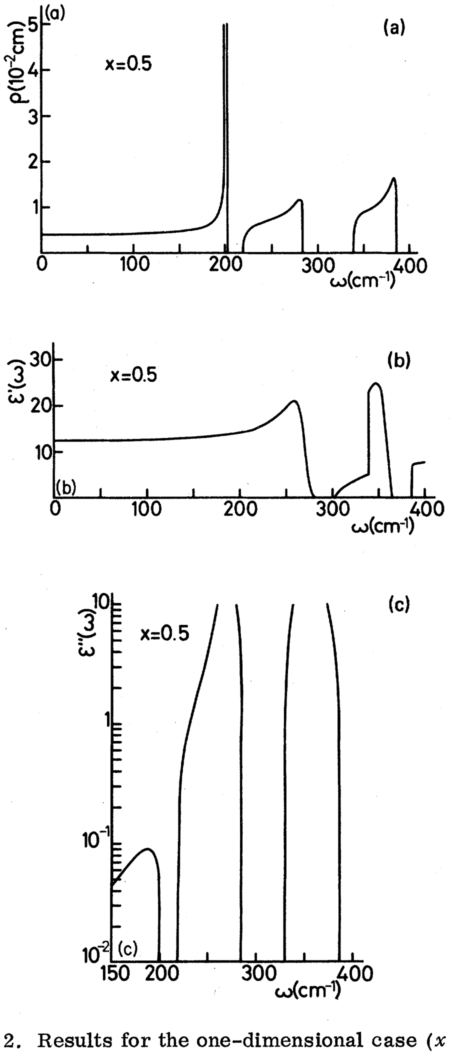

FIG. 2. Results for the one-dimensional case ($x=0.5$). (a) Density of states, (b) $\epsilon'(\omega)$, (c) $\epsilon''(\omega)$ (the logarithmic singularities in ϵ'' have been removed).

trum varies dramatically: A localized mode appears, whose intensity grows with x; simultaneously, the optic band is dostorted, it decreases and gradually generates a gap mode.

The behavior of the dielectric constant ϵ must be examined more carefully. The discontinuities of the one-dimension density of states results in discontinuities in its real part ϵ' [Fig. 2(b)] and simultaneous logarithmic singularities in its imaginary part ϵ'', thus revealing spurious modes one has to eliminate [Fig. 2(c)]. It appears that the ir spectrum evidences the well-known two-mode behavior, evolving from the optical multiplet of the pure GaAs crystal toward the localized mode of Ga in AlAs with decreasing LT splitting, and conversely. On the plotting of $\epsilon''(\omega)$ at various concentrations, one sees that one mode becomes higher and sharper while the other becomes broad and weak. The model also evidences another mode whose position and intensity vary slowly in the whole range of concentrations (except when $x\rightarrow0$ or $x\rightarrow1$). The intensity of this mode is very weak with respect to that of the other ones (about a hundred times) and evidences no LT splitting; its signature upon $\epsilon'(\omega)$ is hardly visible. From its position, one can interpret it as an acoustic zone-edge mode (thus a maximum density of states in this one-dimensional case) optically inactive in a perfect crystal, but made weakly active by the disorder and the contamination by the mode $\vec{k}=\vec{0}$. The results for ω_L, ω_T are given in Fig. 3 (precision of the calculation ~ 0.5 cm^{-1}). Clearly, the tendencies are accounted for, but the numerical values are not excellent (for instance, see in Table II the positions of the localized modes compared with the experimental values extrapolated from Ref. 20), and this is mainly due to the one-dimensional model, as we shall see now.

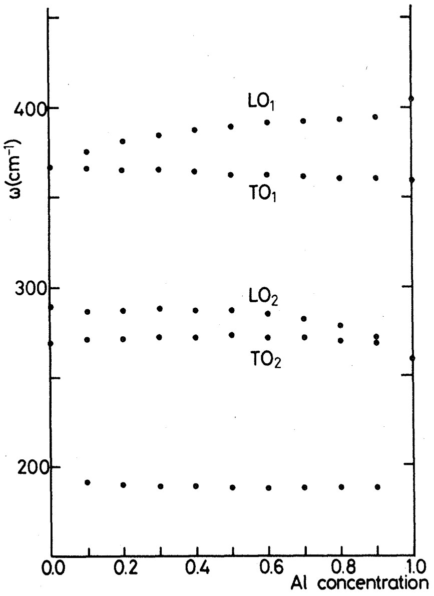

FIG. 3. ω_L and ω_T versus Al concentration in the one-dimensional case.

V. THREE-DIMENSIONAL MODEL

In the three-dimensional case, an exact series expansion of the Green function G_0 can be performed in the range $\omega_M < \omega < \omega_m$ and $\omega > \omega_\mu$ where it is real (see Appendix). This enables one to determine the localized modes of Ga in AlAs and of Al in GaAs. The values are given in Table II and compared with the experimental values (extrapolated from Ref. 20) and those obtained from the one-dimensional model. One sees that an important part of the discrepancy is recovered. Thus, as far as the optical properties are concerned, the single-force-constant model, in spite of its simplicitly, agrees fairly well with the experimental data.

However, such an expansion is not possible in general, and as a consequence, in the continuum limit G is not easy to calculate. Nevertheless the problem of finding the properties of the disordered medium can be handled if one knows the density of states of a reference medium, which is here the virtual crystal, and injects it in the CPA procedure. We have the simple way which is now described.

The density of states

$$D(\omega^2) = \frac{v}{(2\pi)^3} \int_{\omega^2(\vec{k})=\mathrm{const}} \frac{d^3k}{d\omega^2}$$

in our simple model is easily written as

$$D(\omega^2) = \frac{v}{(2\pi)^3} \frac{2\omega^2 - \omega_\mu^2}{\omega_M^2 \omega_m^2} \int_{|\sigma_{\vec{k}}|^2=\mathrm{const}} \frac{d^3k}{d\omega^2} .$$

The one-dimensional density of states $D(\omega^2)$ evidences infinite singularities for $\omega = 0$, ω_M, ω_m, ω_μ, and the two-dimensional density has logarithmic singularites. In the three-dimensional case the density of states is continuous but its derivative is not in a few critical points where $\vec{\nabla}_k(\omega^2) = \vec{0}$. An initial study by Van Hove,[21] restricted to the so-called analytical case where an expansion $\omega^2 = \omega_c^2 + \sum a_{ij} k_j k_j$, with $\det(a_{ij}) \neq 0$ was possible around these points, was later extended by Phillips.[22] In our one-force-constant model, the acoustic band $D_{\mathrm{ac}}(\omega^2)$ has

(i) an analytical singularity in $\vec{k} = \vec{0}$ ($|\sigma_{\vec{k}}|^2 = 1$), such that

$$D_{\mathrm{ac}}(\omega^2) = \begin{cases} \dfrac{12}{\pi^2} \left(\dfrac{M+m}{2K}\right)^{3/2} (\omega^2)^{1/2} & \text{if } \omega > 0 \\ 0 \ \text{if } \omega < 0 , \end{cases}$$

(ii) an analytic singularity in the point L of the Brillouin zone ($\vec{k} = \frac{1}{2}, \frac{1}{2}, \frac{1}{2}$, i.e., $|\sigma_{\vec{k}}|^2 = \frac{1}{4}$), such that

$$D_{\mathrm{ac}}(\omega^2) = \begin{cases} A + B(\omega_L^2 - \omega^2)^{1/2} & \text{if } \omega < \omega_L \\ A \ \text{if } \omega > \omega_L , \end{cases}$$

(iii) a nonanalytic singularity in $\vec{k} = (1, 0, 0)$ and $\vec{k} = (1, 1, 0)$ (i.e., $|\sigma_{\vec{k}}|^2 = 0$, $\omega = \omega_M$), such that

$$D_{\mathrm{ac}}(\omega^2) = \begin{cases} C(\omega_M^2 - \omega^2)^{1/2} & \text{if } \omega < \omega_M \\ 0 \ \text{if } \omega > \omega_M . \end{cases}$$

The behavior of the optic branch is obtained with no further investigation since $D(\omega^2) = D(\omega_{\mu 2} - \omega^2)$. As Phillips has pointed out, the knowledge of the density of states in the vicinity of the critical point gives an excellent approximation of the density of states everywhere by interpolation between

TABLE II. Single impurity modes.

	Expt. (from Ref. 19)	Diatomic chain	Three-dimensional series expansion of the Green function	Three-dimensional approximate density of states
Al:GaAs	350	366.5	351.6	353.2
Ga:AlAs	254	260.0	257.8	255.9

the singularities, the height of the peaks being determined by the normalization condition. We have tested this point by a comparison with a root sampling procedure over 48 × 22 100 points of the Brillouin zone, and the agreement is quite good. We are thus provided with an analytical expression of the density of states of the reference medium. Obtaining the Green function by a Hilbert transform is straightforward, as follows.

To get $\tilde{G}_0^{aa}(z)$ and $\tilde{G}_0^{bb}(z)$ in the CPA [Eq. (15)] we have to compute the sum

$$J=\frac{v}{(2\pi)^3}\int d^3k\,\frac{1}{\tilde{m}Mz^4-2K(\tilde{m}+M)z^2+4K^2(1-|\sigma_{\vec{k}}|^2)}$$

in the continuum limit (v is the volume of the unit cell). For the reference crystal ($\tilde{m}=\bar{m}$), the sum over the Brillouin zone can be straightforwardly written as

$$\frac{1}{\bar{m}M2z^2-2K(\bar{m}+M)}\,\frac{v}{(2\pi)^3}\int d^3k\left(\frac{1}{z^2-\omega_{\mathrm{ac}}^2(\vec{k})}+\frac{1}{z^2-\omega_{\mathrm{op}}^2(\vec{k})}\right)$$

or

$$\frac{1}{\bar{m}M2z^2-2K(\bar{m}+M)}\int d(x^2)\,\frac{D(x^2)}{z^2-x^2}\,.$$

[Let us recall here that $D(x^2)$ is the density of states of the reference crystal (the virtual crystal) and that the contribution of each of the six phonon branches to the density of states, whether degenerate or not, has been normalized to 1.]

Let η be the complex frequency solution of

$$\bar{m}M\eta^4-2K(\bar{m}+M)\eta^2-[\tilde{m}Mz^4-2K(\tilde{m}+M)z^2]=0\,,$$

where by continuity in the limit $\tilde{m}\to\bar{m}$, we keep that of the two solutions whose imaginary part is positive; J is then changed into

$$J=\frac{1}{2\bar{m}M\eta^2-2K(\bar{m}+M)}\int\frac{D(x^2)\,dx^2}{\eta^2-x^2}\,. \tag{30}$$

We can now calculate the density of states and the dielectric function.

The results are shown in Figs. 4–7. The localized modes in the above procedure are similar to those calculated by the analytical expansion of G (Table II), which justify our approximation for $D(\omega^2)$. The density of states (Fig. 4) behaves somehow differently from the one-dimensional case. In the acoustic band, one sees that the Van Hove singularity in the point L of the Brillouin zone has become blunt (since for each value of the wave vector $\vec{k}$ there is an energy band, a kind of broad dispersion curve). There appear two well-defined optical bands with similar shapes; one near the localized mode of Al in GaAs gets higher while the other near the localized mode of Ga in AlAs decreases with greater Al concentration. The band edges exhibit a square root behavior. The CPA solution Y has the behavior shown in Fig. 5: $\mathrm{Re}(Y)$ diverges inside the gap between the two optical bands while $\mathrm{Im}(Y)$ keeps bounded and differs from zero only when $\rho(\omega)$ does. Near $\omega=0$, the acoustic band is well accounted for by the VCA; no doubt that a more elaborate model ($I^{(2)}\neq 0$) would show that the acoustic velocities can be calculated in the VCA as any very low-frequency property. The dielectric function (Figs. 6 and 7) no longer has spurious discontinuities [$\epsilon'(\omega)$ keeps angular points on the band edges]. The weak acoustic zone-edge mode is present; it evidences no LT splitting, and a very broad, very asymmetric profile with a low-frequency tail (the linewidth increase continuously with that of the acoustic band); its frequency varies smoothly and has a minimum at $x=0.7$, its intensity is maximum for $x=0.5$. A more realistic dispersion law with a longitudinal-transverse separation could perhaps remove the degeneracy of this weak mode; let us note that since our model density of states does not reproduce correctly the zone-edge properties, the important point is the predicted existence of this mode, the calculation providing us with only an order of magnitude of its position.

For the two main modes, the longitudinal and transverse frequencies vary nearly linearly when $0.1\lesssim x\lesssim 0.9$, but one has to notice the rapid decrease of the LT splitting between $x=0.0$ and 0.1 and between $x=1.0$ and 0.9, as well for the pure crystal modes and the single impurity modes (Fig. 8); this has been experimentally observed quite recently.[19] The different weight of the longitudinal frequency ω_L and of the transverse one ω_T in the resonance Ω [Eq. (27)] is not sufficient to explain this effect which is due to the disorder (in the same way as the rapid emergence for very low concentrations of the zone-edge mode), and which is revealed by the strong nonlinear character of the CPA equations for weak concentrations. However, in spite of the line broadening, the generalized Lyddane-Sachs-Teller relation

$$\prod_i\left(\frac{\omega_L}{\omega_T}\right)_i^2=\frac{\epsilon_0}{\epsilon_\infty}$$

is verified to better than 2%.

In Fig. 9 we have plotted the maximum heights and the half-height widths of $\epsilon''(\omega)$ and $(-1/\epsilon)''$ for the two main modes. Let us first examine the transverse modes (ϵ''). The lower peak (mainly Ga) linewidth first increases linearly with Al concentration, is maximum near $x=0.7$, then rapidly decreases, whereas its intensity continuously decreases; its shape is slightly asymmetric, decreasing more rapidly on its high frequency side.

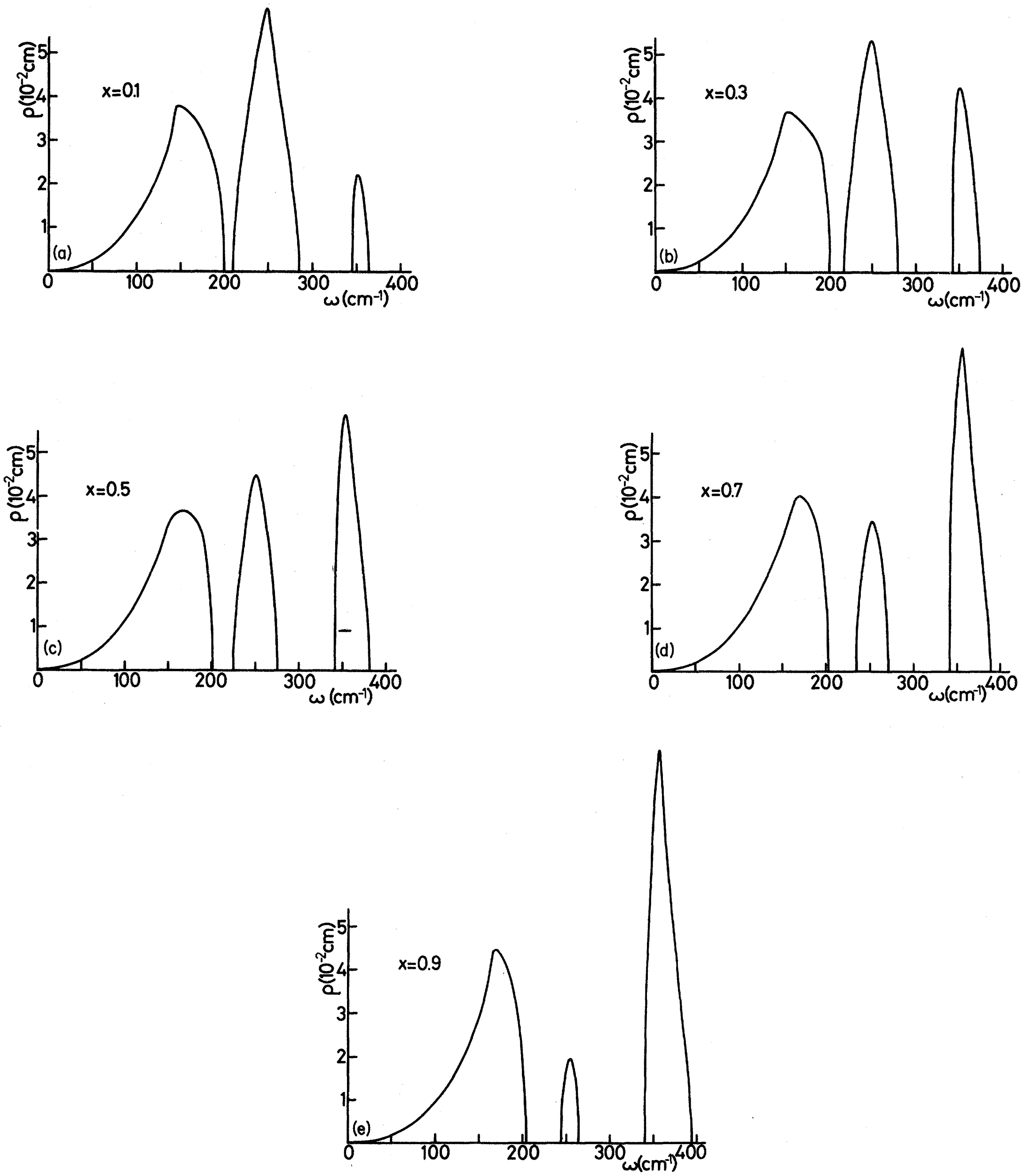

FIG. 4. Three-dimensional density of states for various concentrations.

The upper peak (mainly Al) has an opposite (but not symmetric, due to the mass difference) behavior; for instance, it decreases more rapidly on its low-frequency side. Let us then examine the longitudinal modes $(-1/\epsilon)''$; their intensity and linewidth [Fig. (10)] shows a very rapid variation near the pure-crystal limit; the profiles of the two peaks are strongly asymmetric, abruptly decreasing on the high-frequency side.

Let us conclude with a few words about Raman scattering. In the perfect-crystal case, the frequency and the wave vector of the incident photon $(\omega_I, \vec{k}_I)$, of the Stokes photon $(\omega_s, \vec{k}_s)$, and of the created phonon (ω, k) match in such a way that the conservation laws $\omega_I = \omega_s + \omega$, $\vec{k}_I = \vec{k}_s + \vec{k}$ are satisfied. In the light of what precedes concerning local-field effects, we should instead use the polariton formalism. The dispersion curves of the longitudinal and transverse polariton branches, from which one can compute the polariton density

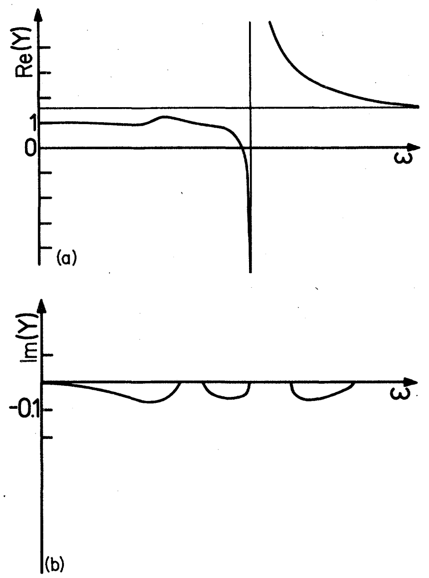

FIG. 5. Behavior of the CPA solution $Y(\omega)$. (a) $\mathrm{Re}(Y)$, (b) $\mathrm{Im}(Y)$.

of states are, respectively, solutions of $\epsilon = (kc/\omega)^2$ and $\epsilon = 0$, where ϵ is given by Eq. (28). In fact, in the wave-vector range of interest, i.e., $k_I - k_s < k < k_I + k_s$, the polariton wave function is almost completely photonlike ($\omega = ck$) or almost completely phononlike; in the latter case, one can safely consider its dispersion as negligible ($\omega = \omega_L$, or $\omega = \omega_T$). (Let us recall a few orders of magnitude: lattice period ~5 Å; visible wavelength ~0.5 μm; phonon wave number ~200 cm^{-1}; the wave vectors of the incident and scattered lights extend to one thousandth of the Brillouin zone and are a hundred times greater than the phonon wave vector.) So as to compute the differential scattering cross section, one has to know the projected density of final states $d(\omega, \vec{k})$, i.e., the number of vibration modes whose wave vector lies between $\vec{k}$ and $\vec{k} + d\vec{k}$, and whose frequency lies between ω and $\omega + d\omega$.

For the transverse (twice degenerate) branch

$$d^T(\omega, \vec{k}) = -\frac{2\omega}{\pi} \frac{v}{(2\pi)^3} \,\mathrm{Im}\, \frac{2}{\omega^2 - z_T^2} ,$$

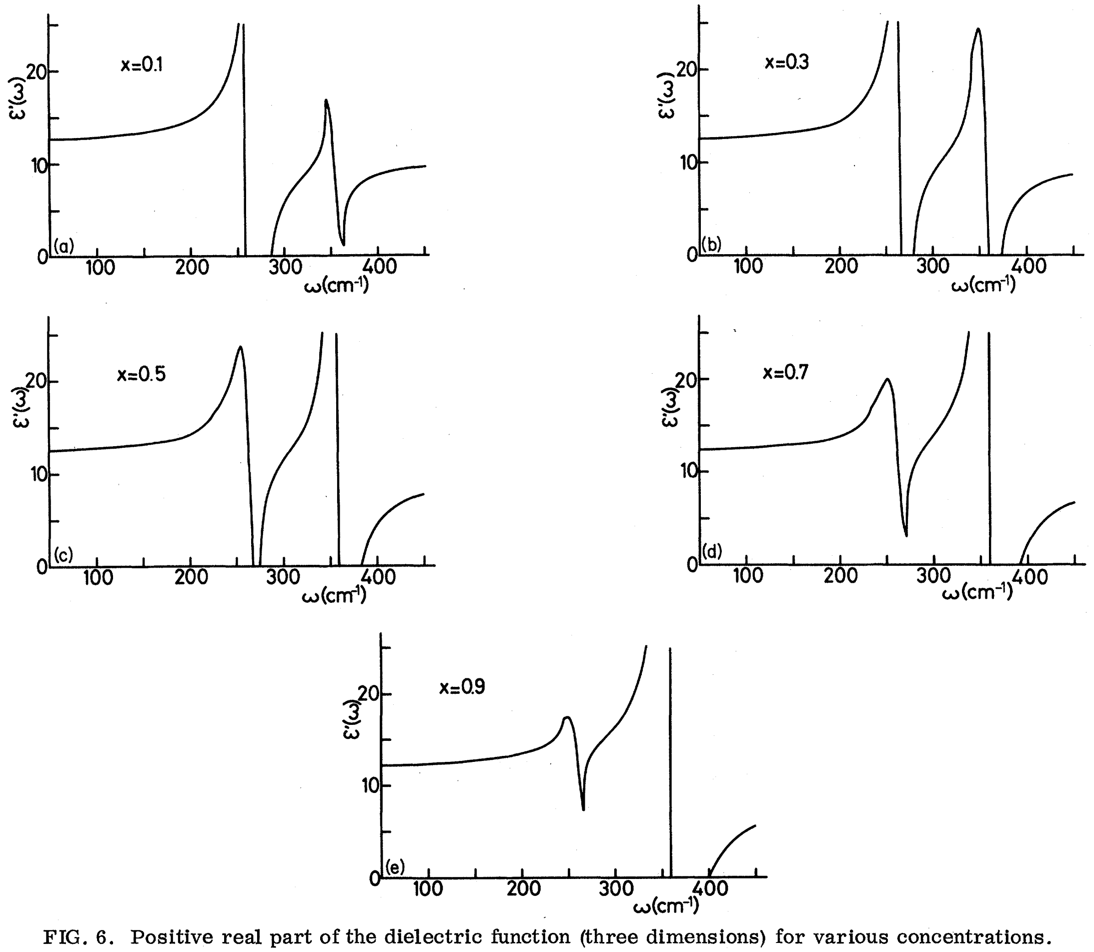

FIG. 6. Positive real part of the dielectric function (three dimensions) for various concentrations.

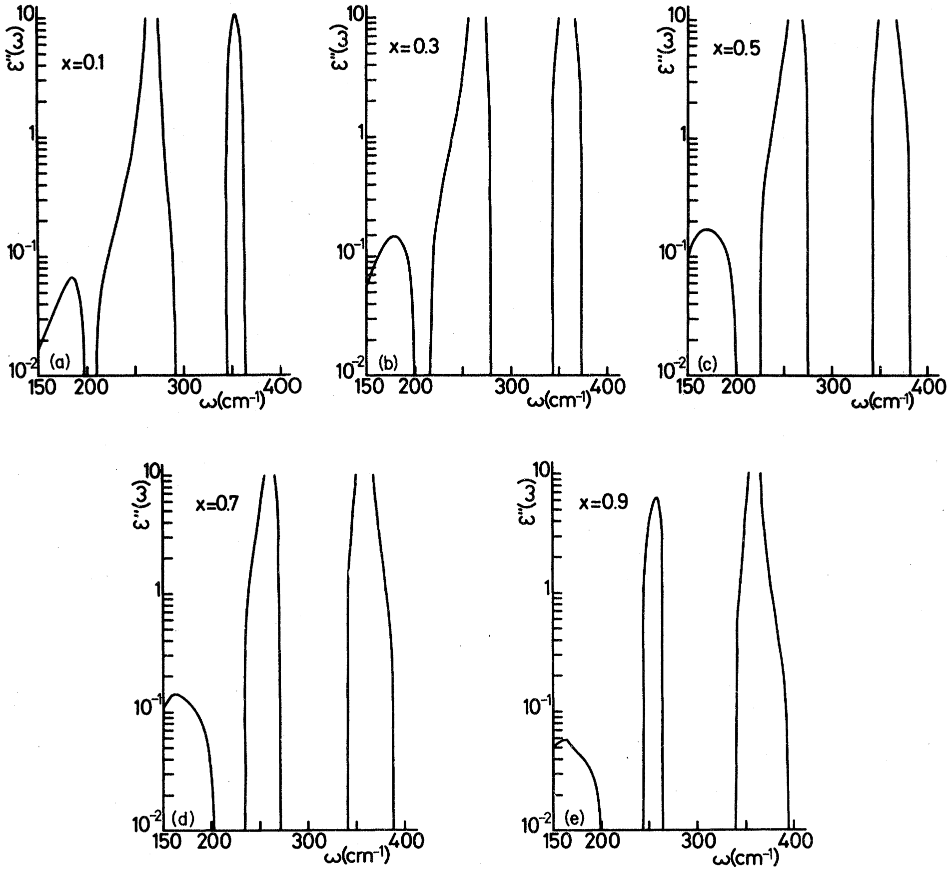

FIG. 7. Imaginary part of the dielectric function for various concentrations (three dimensions).

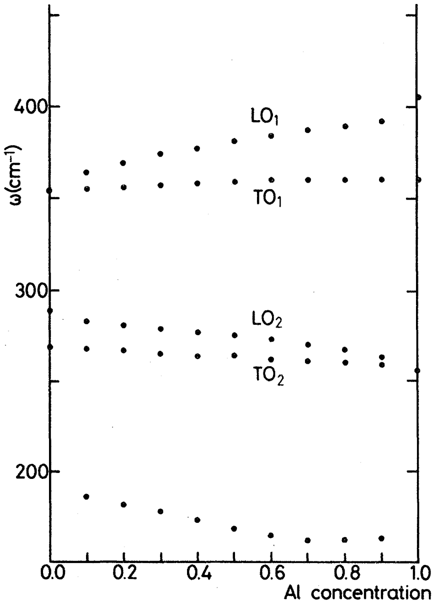

FIG. 8. Plotting of ω_T and ω_L versus Al concentration in the three-dimensional case.

and for the longitudinal branch (no degeneracy)

$$d^L(\omega,\vec{k}) = -\frac{2\omega}{\pi}\frac{v}{(2\pi)^3}\,\mathrm{Im}\,\frac{1}{\omega^2 - z_L^2}\,.$$

The behavior of $d^T(\omega,\vec{k})$ and $d^L(\omega,\vec{k})$ is very similar to that of ϵ'' and $(-1/\epsilon)''$, respectively (position of the maxima, line shape, linewidth). However, the Raman amplitude is also proportional to

$$\frac{\partial \alpha_{ij}}{\partial Q_k}\, Q_k$$

(α_{ij} is the electronic polarizability and Q_k the normal coordinate with wave vector k), and the correlations certainly cannot be neglected when calculating the average intensity which is proportional to $\langle |(\partial\alpha_{ij}/\partial Q_k)Q_k|^2\rangle$. The theory of the Raman effect in an alloy still has to be done.

VI. CONCLUSION

We have presented a simple three-dimensional model of the optical properties of ternary semi-

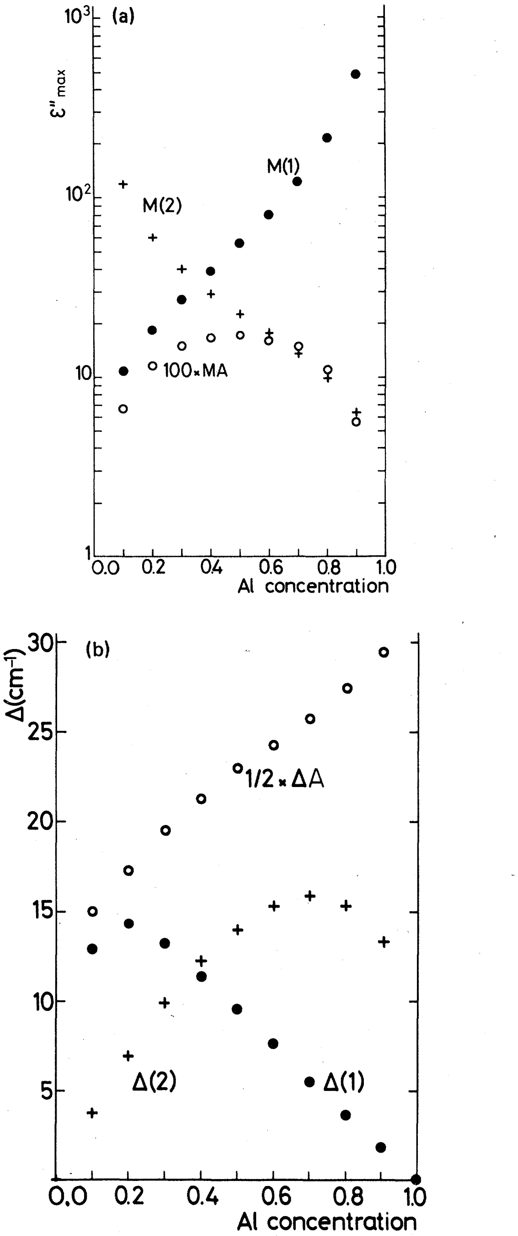

FIG. 9. (a) Peak intensity of ϵ'' [$M(1)$ is the Al mode, $M(2)$ the Ga mode, and MA the acoustic mode result multiplied by 100]. (b) Linewidth [$\Delta(1)$ Al mode, $\Delta(2)$ for the Ga mode, and ΔA for the acoustic mode half-width].

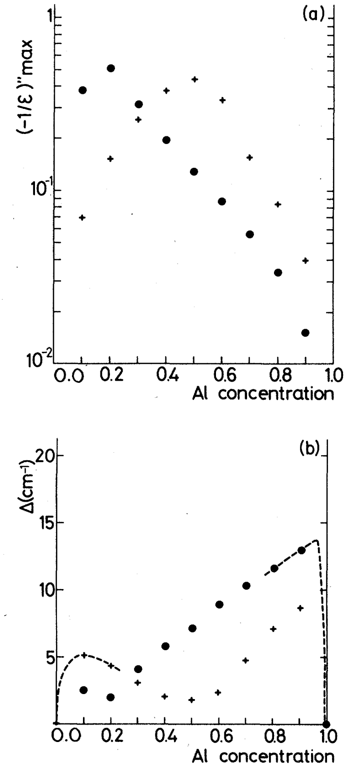

FIG. 10. (a) Peak intensity of $(-1/\epsilon)''$. (● represents the Al mode, and + the Ga mode.) (b) Linewidth.

conductor alloys. We have shown that in spite of its apparent roughness, the isotropic one-force-constant model accounts fairly well for the observed spectra, and makes explicit the problem linked to the local-field corrections without ambiguity. There is no doubt that a more realistic model could give a far better density of states, solve the little discrepancies in the numerical values of the frequencies of the localized modes, and make the behavior of the zone-edge mode more precise, but no doubt also that it would be at the price of a much greater numerical complexity. We think that this model could be applied with no great changes to other quasiboson elementary excitations, such as excitons.

ACKNOWLEDGMENTS

I am very grateful to D. Paquet for numerous and helpful discussions about Green functions and the CPA model. Thanks are due to B. Jusserand and J. Sapriel for communicating experimental results prior to their publication.

APPENDIX

This Appendix aims to show how the Green function $G_0(\omega)$ can be expanded in a series. One introduces the reduced variable

$$T=\frac{\omega_M^2\omega_m^2}{(\omega^2-\omega_M^2)(\omega^2-\omega_m^2)}\,,$$

so that calculating the sums [Eq. (15)] with $\tilde{m}=\bar{m}$ involves computing

$$S=\frac{1}{N}\sum_{\vec{k}}\frac{1}{1-T|\sigma_{\vec{k}}|^2}\,.$$

The expansion

$$S = 1 + T\langle |\sigma_{\vec{k}}|^2\rangle + T^2\langle |\sigma_{\vec{k}}|^4\rangle + \cdots$$

converges if $|T| < 1$, and in particular if $\omega^2 > \omega_\mu^2$. From the expression

$$|\sigma_{\vec{k}}|^2 = \frac{1}{4}\left[1 + \cos\left(\frac{k_x a}{4}\right)\cos\left(\frac{k_y a}{4}\right) + \cos\left(\frac{k_y a}{4}\right)\cos\left(\frac{k_z a}{4}\right) + \cos\left(\frac{k_z a}{4}\right)\cos\left(\frac{k_x a}{4}\right)\right],$$

$|\sigma_{\vec{k}}|^{2N}$ can be expressed as a multinomial expansion

$$|\sigma_{\vec{k}}|^{2N} = \frac{1}{4^N}\sum_{p,q,r,s;\,p+q+r+s=N}\left(\cos\frac{k_x a}{4}\right)^{q+s}\left(\cos\frac{k_y a}{4}\right) \times \left(\cos\frac{k_z a}{4}\right)^{r+q}\frac{N!}{p!q!r!s!}.$$

In the continuum limit,

$$\left\langle\left(\cos\frac{k_x a}{4}\right)^{2m+1}\right\rangle = 0,$$

$$\left\langle\left(\cos\frac{k_x a}{4}\right)^{2m}\right\rangle = \begin{cases} 1 & \text{if } m = 0 \\ \dfrac{1}{2^{2m-1}}\dfrac{(2m-1)!}{m!\,(m-1)!} & \text{if } m \neq 0. \end{cases}$$

So that one obtains

$$S = 1 + \frac{T}{4} + \frac{7}{64}T^2 + \frac{T^3}{16} + \frac{7\times 97}{2^{14}}T^4 + \cdots.$$

One can also introduce the reduced variable

$$R = \frac{\omega_M^2\omega_m^2}{\omega^2(\omega^2 - \omega_\mu^2)} = \frac{T}{1 - T}.$$

One has then to compute

$$S' = \frac{1}{N}\sum_{\vec{k}}\frac{1}{1 + R(1 - |\sigma_{\vec{k}}|^2)},$$

which can be expanded as

$$S' = 1 - R\langle 1 - |\sigma_{\vec{k}'}|^2\rangle + R^2\langle (1 - |\sigma_{\vec{k}'}|^2)^2\rangle + \cdots,$$

if $|R| < 1$, and in particular if $\omega_M^2 < \omega^2 < \omega_m^2$.

Using the previous results, one obtains

$$S' = 1 - R\ \ 1 - \tfrac{1}{4}\ \ + R^2\ \ 1 - \tfrac{2}{4} + \tfrac{7}{64}) + \cdots$$

$$= 1 - \tfrac{3}{4}R + \tfrac{21}{32}R^2 + \cdots.$$

Finally, one has

$$\sum_{\vec{k}}\frac{1}{\omega^4 - \omega^2(\omega_M^2 + \omega_m^2) + \omega_M^2\omega_m^2(1 - |\sigma_{\vec{k}}|^2)} = \frac{S}{(\omega^2 - \omega_M^2)(\omega^2 - \omega_m^2)},$$

or alternatively, $S'/\omega^2(\omega^2 - \omega_\mu^2)$.

---

*Division RPC, Laboratoire associé au CNRS (LA 250).

[1] M. Born and K. Huang, *Dynamical Theory of Crystal Lattices* (Oxford University Press, New York, 1968).

[2] A. S. Barker Jr. and A. J. Sievers, Rev. Mod. Phys. 47, S1 (1975) and references herein.

[3] A. A. Maradudin, P. Mazur, E. W. Montroll, and G. H. Weiss, Rev. Mod. Phys. 30, 175 (1958).

[4] I. F. Chang and S. S. Mitra, Adv. Phys. 20, 359 (1971).

[5] P. Mazur, E. W. Montroll, R. B. Potts, and J. Wash, Acad. Sci. 46, 2 (1956).

[6] E. W. Montroll and R. B. Potts, Phys. Rev. 100, 525 (1955); 102, 72 (1956).

[7] R. J. Elliott and D. W. Taylor, Proc. R. Soc. London (1967).

[8] R. J. Elliott, J. A. Krumhansl, and P. L. Leath, Rev. Mod. Phys. 46, 465 (1974).

[9] D. W. Taylor, Phys. Rev 156, 1017 (1967).

[10] P. Dean, Rev. Mod. Phys. 44, 127 (1972).

[11] P. N. Sen and W. M. Hartmann, Phys. Rev. B 9, 367 (1974).

[12] T. Kaplan and M. Mostoller, Phys. Rev. B 9, 353 (1974).

[13] P. Soven, Phys. Rev. 156, 809 (1967); 178, 1136 (1969).

[14] R. Bonneville and G. Fishman, Phys. Rev. B 22, 2008 (1980); the determination of the exchange energy from the available experimental data can be altered up to an order of magnitude. Also, R. Bonneville, Phys. Rev. B 21, 368 (1980).

[15] F. J. Dyson, Phys. Rev. 92, 1331 (1953).

[16] Putting $I^{(1)} = I^{(2)}/2$, Eq. (11) becomes equivalent to the Thorpe and Weaire model [Phys. Rev. B 4, 3518 (1971)], which caused LO and LA dispersed modes but TO and TA flat branches; $I^{(0)} = 0$ causes an LT splitting, but trivial ($\omega = 0$) optical modes.

[17] P. N. Sen and G. Lucovsky, Phys. Rev. B 12, 2998 (1975).

[18] If $\gamma = 1$, Eq. (22) involves the Clausius-Mossoti formula

$$\epsilon_\infty - 1 = \frac{4\pi\frac{N}{V}\alpha_\infty}{1 - \frac{4\pi}{3}\frac{N}{V}\alpha_\infty},$$

where as the case $\gamma = 0$ leads to the Darwin formula $\epsilon_\infty - 1 = 4\pi(N/V)\alpha_\infty$.

[19] B. Jusserand and J. Sapriel, unpublished.

[20] R. Tsu, H. Kawamura, and L. Esaki, in *Proceedings of the Eleventh International Conference on the Physics of Semiconductors, Warsaw, 1972,* edited by M. Miasek (PWN–Polish Scientific, Warsaw, 1972), Vol. II, p. 1135.

[21] L. Van Hove, Phys. Rev. 89, 1189 (1953).

[22] J. C. Phillips, Phys. Rev. 104, 1263 (1956).